International Conference on Flood Resilience:
Experiences in Asia and Europe
5-7 September 2013, Exeter, United Kingdom

MACHINE LEARNING-BASED EARLY WARNING SYSTEM FOR URBAN FLOOD MANAGEMENT

Andrew P. Duncan[1,*], Edward C. Keedwell[1], Slobodan Djordjević[1], Dragan A. Savić[1]

[1] University of Exeter, United Kingdom
[*] *Harrison Building, North Park Road, Exeter, EX4 4QF, United Kingdom; Tel: +44 (0)1392 724075; E-mail: apd209@exeter.ac.uk*

ABSTRACT

With the growth in urban population and other pressures, such as climate change, the impact and severity of urban flood events are likely to continue to increase. "Intelligent water networks" are viewed as the way forward to ensure that infrastructure services are flexible, safe, reliable and economical. Reduction of flood-risk from urban drainage and sewerage infrastructure is likely to require increasingly sophisticated computational techniques to keep pace with the level of data that is collected both from meteorological and online water monitoring systems in the field. This paper describes and characterises an example of an Early Warning System (EWS), designated "RAPIDS" (RAdar Pluvial flooding Identification for Drainage System) that deals with urban drainage systems and the utilisation of rainfall data concurrently to predict flooding of multiple urban areas in near real-time using a single multi-output Artificial Neural Network (ANN). The system has the potential to provide early warning for decision makers within reasonable time, this being a key requirement determining the operational usefulness of such systems. Computational methods that require hours or days to run will not be able to keep pace with fast-changing situations such as manhole flooding or Combined Sewer Overflow (CSO) spills and thus the system developed is able to react in close to real time. This paper includes a sensitivity analysis and demonstrates that the - predictive capability of such a system based on actual rainfall is limited to a maximum of the Time of Concentration (ToC) of each node being modelled. To achieve operationally useful prediction times, predictions of rainfall as input signals are likely to be needed for most urban drainage networks.

KEYWORDS
Artificial neural network; climate change; early warning system; flood prediction; time of concentration; urban flooding.

1. INTRODUCTION

As referred to in our earlier paper (Savić et al., 2013), today, half of the world's population lives in cities and, by 2030, this will grow to nearly 60% (Heilig, 2012). The trends in urban population growth together with other pressures, such as climate change, create enormous challenges to provision of resilient and safe urban drainage services despite, in many cases, ageing infrastructure. Urban drainage management involves consideration of sustainable use of water resources, pollution control, stormwater and wastewater network management and flood control and prevention. The high costs of expanding, renewing and strengthening the physical infrastructure to relieve these pressures mean there is a critical and urgent need to investigate and implement 'intelligent' management techniques toward improved use of the existing urban water infrastructure. This may help delay many large infrastructure investments otherwise required to mitigate urban flood-risks.

"Intelligent grid" and/or "smart grid" are terms that have their origin in the electricity industry (Amin and Wollenberg, 2005). They refer to an electrical grid that uses information and communications technology (ICT) to automate processes that improve the efficiency, reliability, economics and sustainability of the production and distribution of electricity. This concept of smart-grid technology is being adopted in many countries around the world as the way forward to ensure that electricity networks are flexible, accessible, reliable and economical (European Commission, 2006). The intelligent grid concept will also benefit from the rapid increase in the amount of data (i.e., "big data") becoming available through proliferation of sensors, mobile communications, social media, etc. However, without intelligent computational methods, grid managers and decision makers will find it increasingly difficult to make sense of the large amount of data being made available in near real-time.

In a similar vein to the smart electricity grid, “intelligent water networks” or “intelligent water infrastructure”, which take advantage of the latest ICT to gather and act on information in an automated fashion, could allow the minimisation of waste and delivery of more sustainable water services. This paper describes and analyses an example of machine learning-based intelligent systems developed to utilise increasingly available real-time sensor information in the urban water environment. It deals with urban drainage systems and utilises rainfall data to predict flooding for multiple urban locations in near real-time. Currently, observation data from urban drainage networks is still fairly sparse, but there is no need to wait for online monitoring "big-data" to become universally available; rapid real-time predictive models can be created and studied as data-driven surrogates of much slower and computationally demanding hydraulic or hydrodynamic models. These latter typically take rainfall hyetographs as input and produce flood level / volume / flow hydrographs for sewerage nodes as output, based on a parameterised physical model of a sewerage network and a set of physically-based equations describing the water flow into, through and out of the network (Zoppou, 2001).

Early Warning Systems (EWS), in order to be operationally useful, need to provide at least a 2-hour lead-time (Einfalt et al., 2004; UKWIR, 2012). However, for large networks and/or when repetitive simulation runs are needed (i.e., for flood risk assessment), these can be slow and computationally expensive. We present a faster surrogate method based on Artificial Neural Networks (ANN) that permits modelling of very large drainage networks in real-time, without unacceptable degradation of accuracy. It should be noted that because these are not physical models, there is no need to model every sewerage node; it is sufficient to model only those nodes identified from the output of the physical model as having a probability of flooding above some threshold value: "key" nodes. Furthermore, in the case of the trained feedforward ANN's used in this study, there are no iterative loops; predictive outputs are obtained directly from a non-linear combination of time-lagged inputs. These two factors combine to produce considerable computational cost saving and hence speed improvement when compared to physically-based hydrodynamic models.

1.1 Artificial Neural Networks for Urban Flood Modelling

As part of University of Exeter’s contribution to research under the Flood Risk Management Research Consortium Phase 2 (FRMRC2, 2011; Schellart et al., 2011) project and the UK Water Industry Research (UKWIR, 2012) follow-on case studies, RAPIDS was developed using a single, multi-output ANN to predict flooding at multiple nodes in sewer systems (Duncan et al., 2011, 2013). This paper assesses the opportunities provided by data-driven ANN-based models for rapid and concurrent predictions of urban flooding from manholes and Combined Sewer Overflow (CSO) spills at multiple locations in a sewerage network. This could provide water utilities and local authorities with the ability to improve their level of service and compliance with regulation as well as reduce risks to their customers and the general public, through taking effective action to mitigate impacts of flooding.

The sensitivity analysis described here shows that, when based on actual rainfall as input, the predictive ability of time-lagged ANNs is limited to of the order of the delay of the peak of cross-correlation between the rainfall input hyetograph and the hydrograph for each given node in the sewer network. This approximates to the Time of Concentration (ToC) for each node, when measured for the longest duration rainfall events. ToC describes the maximum transit time of water from the furthest (upstream) point of the urban catchment to the given node (Butler and Davies, 2004). With the exception of the most downstream nodes in the very largest urban drainage networks, this would normally be very short, i.e., of the order of tens of minutes, rather than hours, thus requiring prediction of rainfall to achieve the required operational lead-times. Rainfall nowcasting (forecasting <6 hours ahead) is commonly obtained from radar rainfall images (Schellart et al., 2009; Wang et al., 2009). Although work has been carried out with the UK Met Office Nimrod 1km composite radar images (with 5-minute temporal resolution) and Environment Agency telemetered raingauge network (with 15-minute temporal resolution) (UKWIR, 2012), in this study we present results based on synthetic design rainfall events using a range of return periods and durations for Portsmouth, UK.

Due to the lack of measured data from urban flooding events for the case-study urban drainage network of Portsmouth, UK, the InfoWorks CS model (Innovyze, 2012) is used as a surrogate, so as to provide time-series (hydrographs) describing system performance at manholes, CSOs and outfalls. ANN models are then developed to predict performance at these key points of interest for any rainfall loading condition and these predictions are compared to InfoWorks CS results, which are treated as 'ground truth' for the purposes of the study. During training of the ANN model, they represent the target signals and during system test they represent reference signals against which to evaluate the predictive error.

1.2 The ANN model

The ANN model is based on a 2-layer, fully-connected, feedforward Multi-Layer Perceptron (MLP) (Ivakhnenko, 1971; Rumelhart, 1986). This is now an established machine-learning technique applied to many fields. In the case of supervised learning, it relies on the discovery of a multi-dimensional non-linear relationship between the desired model target outputs and a set of predictors (factors) applied as input signals to the model. In applications such as urban flooding, the inputs and targets take the form of time-series signals, sampled at a regular time interval ('timestep'). The modelled relationship is discovered during a 'training' phase based on a number of events from the previous history of the system. Having learnt this generalised relationship, the trained model is then ready for use on new "test" events including those occurring in a live real-time scenario. Although the training process can require significant computational time, the resulting trained ANN model is able to provide flooding responses to rainfall in a fraction of the time required by traditional mathematical models. The fundamental building block of the ANN is the neuron, which has a number of analogue inputs and one output and implements the transfer function:

$$y = f(x) = \kappa\left(\left(\sum_i w_i g_i(x)\right) + b\right) \tag{1}$$

where: x is the input, $g_i(x)$ is some function of x, implemented by the neuron(s) towards the input of the network (for the first layer $g_i(x)=x$), w_i is a weight associated with input i, b is a time-invariant bias level and κ is an activation function applied to the output of the neuron. This might typically implement the hyperbolic tangent (*tanh*), a threshold switch or a linear function. The activation function is selected based on the type of data being processed and so selection is problem-specific for output neurons (e.g. a threshold switch will output an all-or-nothing response whereas the linear and hyperbolic tangent functions will output floating point values).

Figure1 illustrates a 3-layered feed-forward ANN, which is fully-connected within each layer. It should be noted that the input layer simply distributes inputs to all neurons in the hidden layer so there are only 2 layers of neurons.

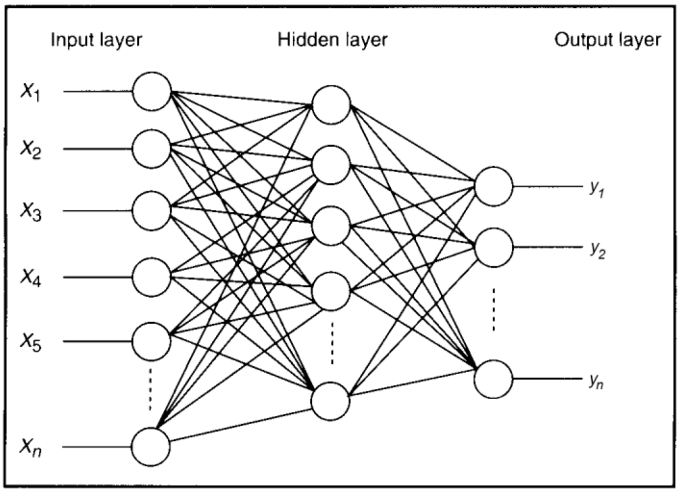

Figure1. Three-layered feedforward ANN

[source: http://mechanicalforex.com/wp-content/uploads/2011/06/NN.png]

In the ANN used, the number of output neurons is given by the number of key nodes in the drainage network. These are typically manholes, CSO's or outfalls. A *tanh* (i.e. non-linear) activation function is used by the hidden layer neurons in order to facilitate modelling of the non-linear processes relating the inputs to the outputs. Because the production of hydrographs involves regression rather than classification, the output neurons use a linear activation function, providing a direct analogue of water level as output. The number of neurons in the hidden layer and number of input nodes are varied to establish an optimum. Batch-mode supervised training is employed, in which expected target data are known for a given set of input data and at each epoch (step) in the training process, the entire training dataset of input samples is presented to the ANN. Target data (output from the InfoWorks CS model) are compared to the output generated by the ANN and errors back-propagated towards the input, adjusting ANN weights and biases so as to reduce the output error. Error optimisation strategies include Scaled-Conjugate-Gradients (SCG), Levenberg-Marquardt (LM) and Quasi-Newton (QN), (Battiti, 1992; Møller, 1993; Hagan and Menhaj, 1994), which are gradient-based approaches.

2. METHODOLOGY

2.1 Input data preparation

A moving time-window lagged approach (Luk et al., 2000; Campolo, 2003; Bowden et al., 2005; Fernando et al., 2005) is implemented. A number of time-series signals (e.g., rainfall intensity, cumulative rainfall during event, etc.) are provided as inputs to the ANN. In the study presented here there are three input time-series: rainfall intensity (mm/hour), cumulative rainfall (mm) and the New Antecedent Precipitation Index (NAPI) value (metres) (Anctil et al., 2004) – a derived measure of soil moisture. The number of input nodes is given by the number of input time-series signals x number of lagged timesteps in the moving input time window. All lags within the window are used, due to the different dependencies that may arise across all the model outputs due to the range of ToC's for the corresponding sewerage nodes.

The trial described is based on sixteen design rainfall events of durations from 0.5, 1, 2 or 4 hours and return periods of 1, 5, 20 or 50 years. Of these, 4 were used as test events and the remaining 12 were used as the training events. All use Laplacian rainfall intensity profiles. Table 1 details the design events used.

Table 1. Matrix of design rainfall events for Portsmouth

Event No	Event Type	Return Period	Duration	Event Use	Event ID
	Design / Real	rrr (Years)	d.dd (Hours)	Trg / Tst	Format rrrddd
1	Design	1	0.5	Trg	001050
2	Design	1	1	Tst	001100
3	Design	1	2	Trg	001200
4	Design	1	4	Trg	001400
5	Design	5	0.5	Trg	005050
6	Design	5	1	Trg	005100
7	Design	5	2	Tst	005200
8	Design	5	4	Trg	005400
9	Design	20	0.5	Trg	020050
10	Design	20	1	Tst	020100
11	Design	20	2	Trg	020200
12	Design	20	4	Trg	020400
13	Design	50	0.5	Trg	050050
14	Design	50	1	Trg	050100
15	Design	50	2	Tst	050200
16	Design	50	4	Trg	050400

Figure 2 is for a 1-hour duration design rainfall event of a 20-year return period for the Portsmouth catchment. This is shown highlighted as Event 14 in Table 1. It shows both inputs (as hyetographs downwards from top) and target signals (as water level hydrographs) for a selection of 10 CSO's and 6 manholes used in this study.

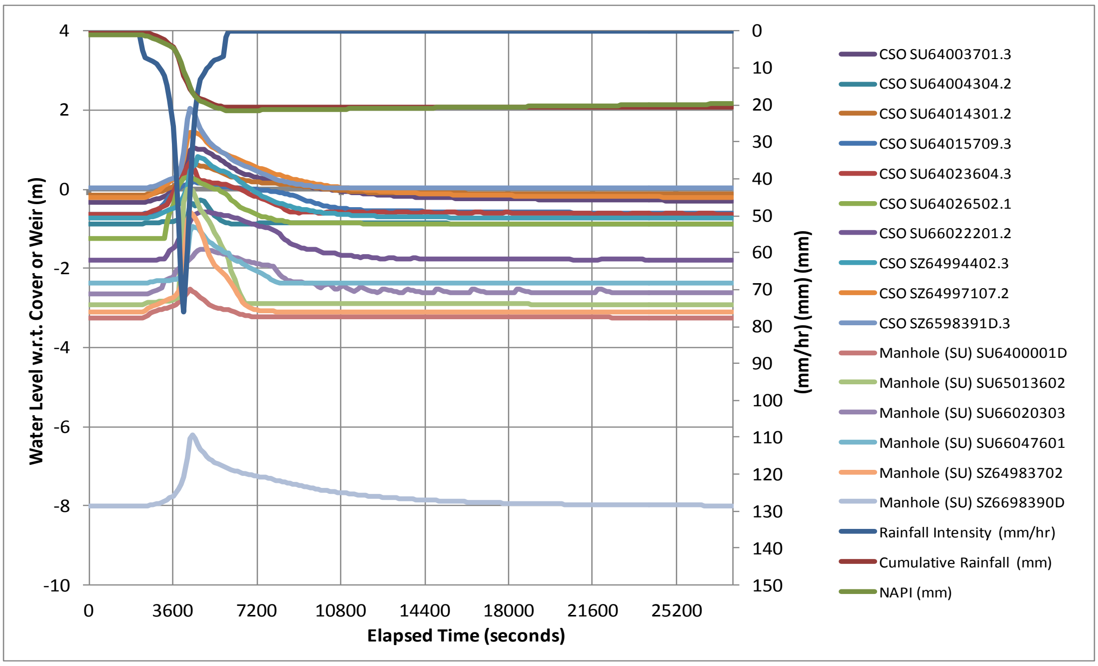

Figure 2. Design rainfall test event (RP=20 years; Duration=1 hour) for Portsmouth catchment

In order to evaluate the ToC's for these nodes, cross-correlations were computed between each rainfall intensity hyetograph and the corresponding 16 hydrographs for a range of delays of the rainfall signal 0 to 3600 seconds. The delays corresponding to the peak of cross-correlation were taken in the case of each node as an approximation to ToC for the event. Figure 3 illustrates this for the above example test event.

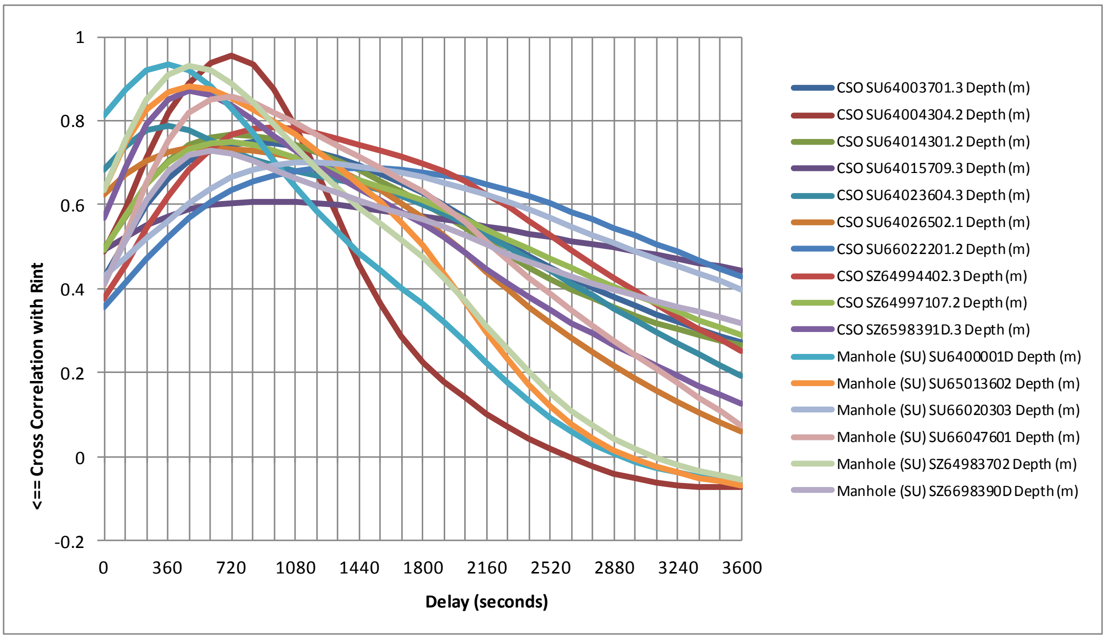

Figure 3. Cross-correlation functions for a set of sewer nodes over a range of delays 0-1 hour for design rainfall test event (RP=20 years; Duration=1 hour) for Portsmouth catchment

Cross-correlations were computed for all events and the spreads of the delay values of the peaks of these are shown in Figure 4 for each sewer node to be included in the ANN model. These are ranked in order of increasing maximum delay value, which can be taken as an approximation to the true time of concentration (Butler and Davies, 2004) for each node. However, in this study we use the actual delays for each event and each node.

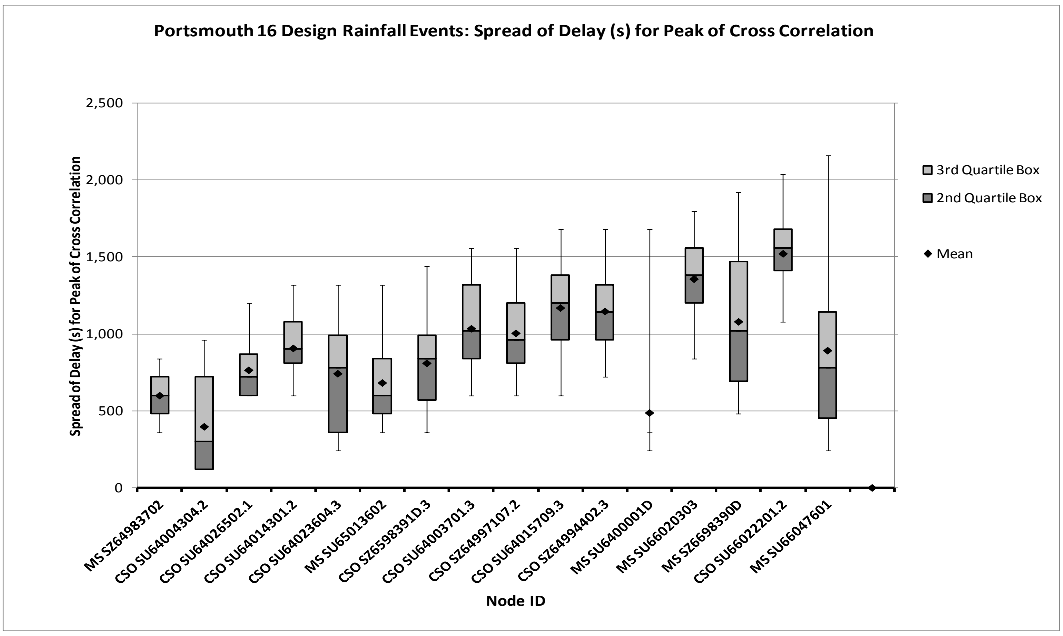

Figure 4. Spreads of cross-correlation peak delays (seconds) for a set of sewer nodes over 16 design rainfall events for Portsmouth catchment

For the 16 nodes from the Portsmouth catchment used in this case study, values of cross-correlation peak delay were between 6 and 35 minutes, with a median of 14.0 minutes. These are taken as indicative of the range of ToC's for these nodes.

2.2 Metrics for evaluation of ANN performance

Results using two metrics are presented. First, in order to evaluate overall performance of each ANN output node over the first 5 hours of the hydrograph for each event, the Nash Sutcliffe Efficiency Coefficient (NSEC) is computed (Nash and Sutcliffe, 1970). The formula used is identical to that published in Moriasi et. al. (2007). Second, in order to evaluate the combined time and amplitude error of the peak of each hydrograph a metric is developed:

$$TA_{err} = (t_t - t_m) * (d_t - d_m) \tag{1}$$

where: TA_{err} = time-amplitude error (metre minutes); t_t = time of peak of target (observed) hydrograph (minutes); t_m = time of peak of modelled ANN output hydrograph (minutes); d_t = water depth of peak of target (observed) hydrograph (metres); d_m = water depth of peak of modelled ANN output hydrograph (metres). This is chosen as an operationally important measure, since it is closely related to the error in predicting the impact of flooding / CSO spills.

The time-amplitude error TA_{err} is illustrated by the area of the shaded rectangle in figure 5. In this case the ANN is shown under-predicting the peak depth (amplitude) and predicting the peak occurring 32-minutes late. This gives TA_{err} = -14.7 for a prediction advance of 30-minutes and a ToC of 14.0-minutes for this node and event. i.e. PTA/ToC=2.14, which is discussed in section 3.2. It is worth noting that despite this poor performance, the NSEC for the first 5-hours of the hydrograph is 0.830, an acceptably high score, indicating the necessity of this second evaluation metric.

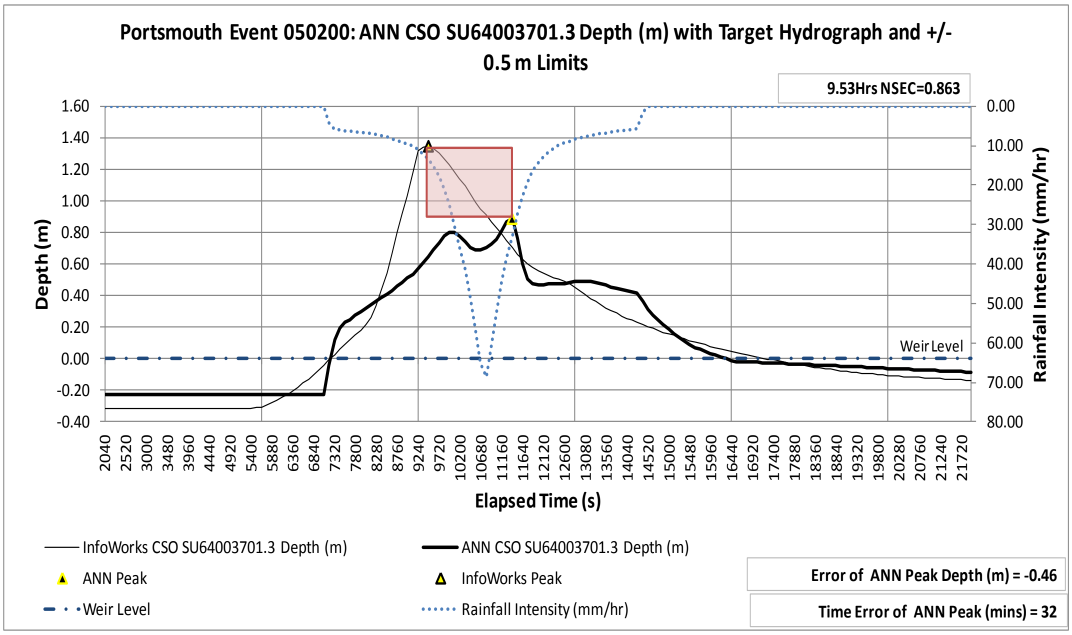

Figure 5. Illustration of time-amplitude error metric for 30-minute prediction advance

2.3 Optimisation of ANN architecture

A single ANN with one output node for each of the 10 CSO's and 6 Manholes is used to predict hydrograph flood/spill depths. For the optimisation process, a single prediction timestep advance (PTA=120s) is used. Two architecture parameters need to be set for optimum model performance, whilst maintaining a parsimonious architecture:

- Number of timesteps lag in the moving input time window ('NIN')
- Number of neuron units in the hidden layer ('NHU')

A range of ANN's using combinations of values: NIN=[1,3,6,9,12,15,18,21,24,30] and NHU=[3,6,10,15,20,30,40,60] are trained using the same 12 rainfall events (see Table 1). During training the performance metric used is mean-squared error (MSE) with a regularisation term to penalise high values of sum-of-squares of neuron weights. This helps to reduce problems with overfitting (Han et al., 2007; Bishop, 2008). Early stopping is also used for the same reason. Prior to training the ANN weights and biases are initialised to different random values, to help demonstrate robustness in the method. Following training of each ANN, NSEC scores are computed for each node and each of the 4 test events. The optimum ANN architecture is then established by looking at the spreads of these for all node outputs and choosing the combination with lowest NIN and NHU without significant degradation of performance. The TA_{err} metric is not used at this stage because performance at PTA=120s (1-timestep advance) is sufficiently good that it is unable to discriminate between good and poor ANN architectures.

2.4 Prediction timing trial

Using the optimum ANN architecture, a timing trial is then performed evaluating NSEC and TAerr performance for each value of prediction timestep advance (PTA) from 0 timesteps to 30 timesteps (1 hour). For each value of PTA a new ANN is trained as above and then the metric performance assessed using each of the 4 test rainfall events. Results are analysed re-scaling the x-axis (PTA) as a proportion of the cross-correlation delay (approx ToC) for each node and for each event.

3. RESULTS & DISCUSSION

3.1 Optimisation of ANN architecture

Figures 6 and 7 show ranges of NSEC scores for a prediction advance of 1-timestep (120s) for all nodes for the shown combinations of NIN and NHU used in the ANN architecture. *Note: minima have been truncated at zero for purposes of the charts*. From this, values around NHU=20 for hidden units performed best, over a wide range of values of NIN (moving time window timesteps), suggesting that this would be a robust value to use.

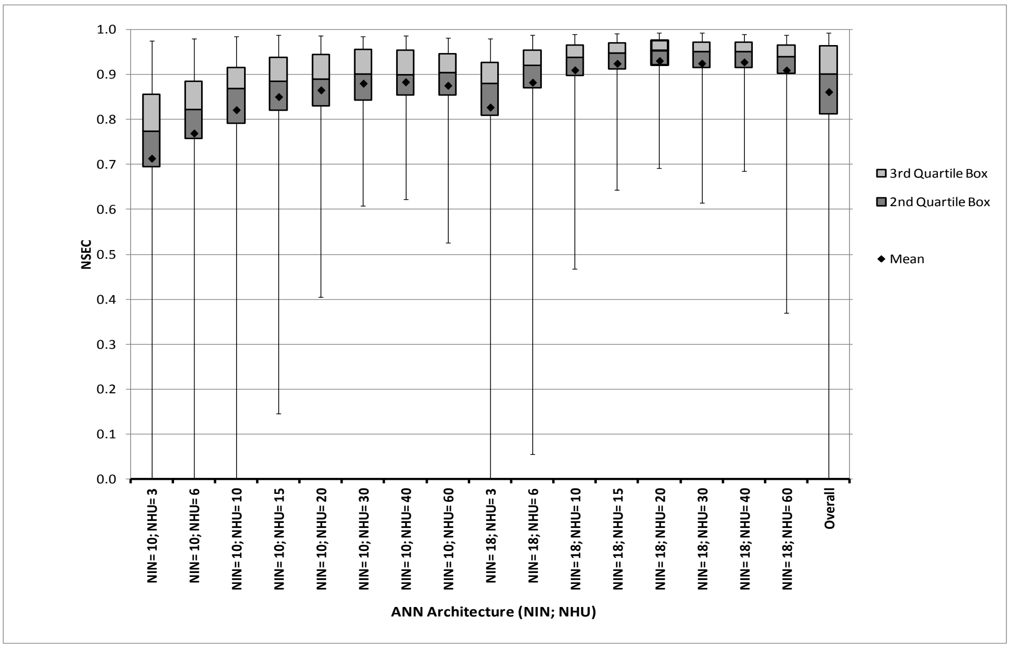

Figure 6. Portsmouth 4 test design rainfall events: Spread of NS scores for NIN=10 and 18 and various NHU values of ANN architecture

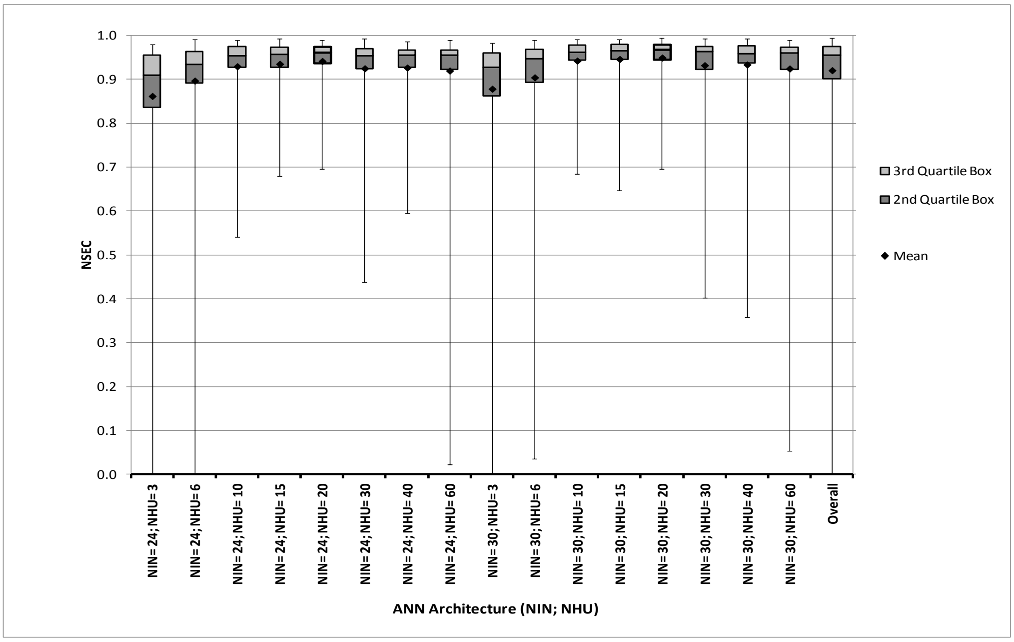

Figure 7. Portsmouth 4 test design rainfall events: Spread of NS scores for NIN=24 and 30 and various NHU values of ANN architecture

Although the ANN's using NIN=30 performed best, those with NIN=18 did not perform significantly worse using a 95% confidence interval (p>0.08). Values of NSEC for NIN=18 and NHU=20 were above 0.69 in all cases, with a median value of 0.95 across all nodes and all 4 test events. Moriasi (2007), reviewing use of the NSEC metric in hydrology, states that NSEC>0.5 is generally taken to represent a "good" model although our UKWIR (2012) study used NSEC>0.85.

3.2 Prediction timing trial

Using the optimised ANN architecture of NIN=18 and NHU=20, the following results were produced for the timing trial described in section 2.4.

Figure 8 analyses the NSEC scores for each node as PTA is increased from zero to 60-minutes. Note: Each value of prediction advance is based on a different ANN, trained by advancing the target signals by that time-interval. In the chart, the x-axis has been re-scaled to normalise to the ToC for each node, such that an x-value of 1.0 is for PTA = ToC for that node. Values above 1.0 are for prediction advances greater than time-of-concentration for the node and *vice versa*. Figure 8 shows the results for the 5-year RP, 2-hour duration design rainfall event.

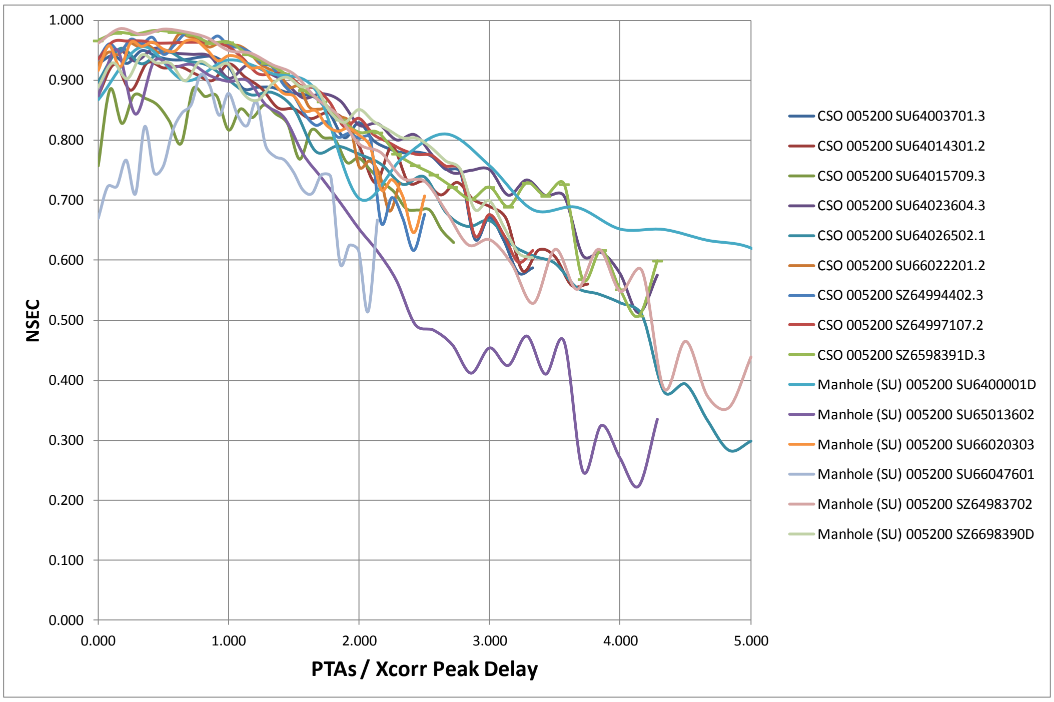

Figure 8. NSEC scores versus ratio of Prediction Timestep Advance to ToC for 5-yr, 2-hr event for 16-nodes from Portsmouth catchment

This clearly demonstrates acceptable performance for PTA less than or equal to 1.0 x ToC and degrading performance for prediction advances above this value. In some cases NSEC performance actually improves towards PTA=ToC then degrades again above this level. This is to be expected, since when PTA=ToC, the peaks of rainfall and hydrograph are perfectly synchronised, making the simplest possible relationship between ANN inputs and outputs. Results for the other 3 test rainfall events are similar, but are not included here due to lack of space.

Figure 9 presents a similarly-formatted chart for the second metric: TA_{err} for the same rainfall event. This shows an even clearer degradation of performance for PTA above 1.0 x ToC. Figure 10 is for the 1-year return period, 1-hour duration event and again illustrates good performance for PTA<=ToC, but demonstrates the tendency for ANNs to overpredict less severe events as its performance breaks down for the longer prediction advances.

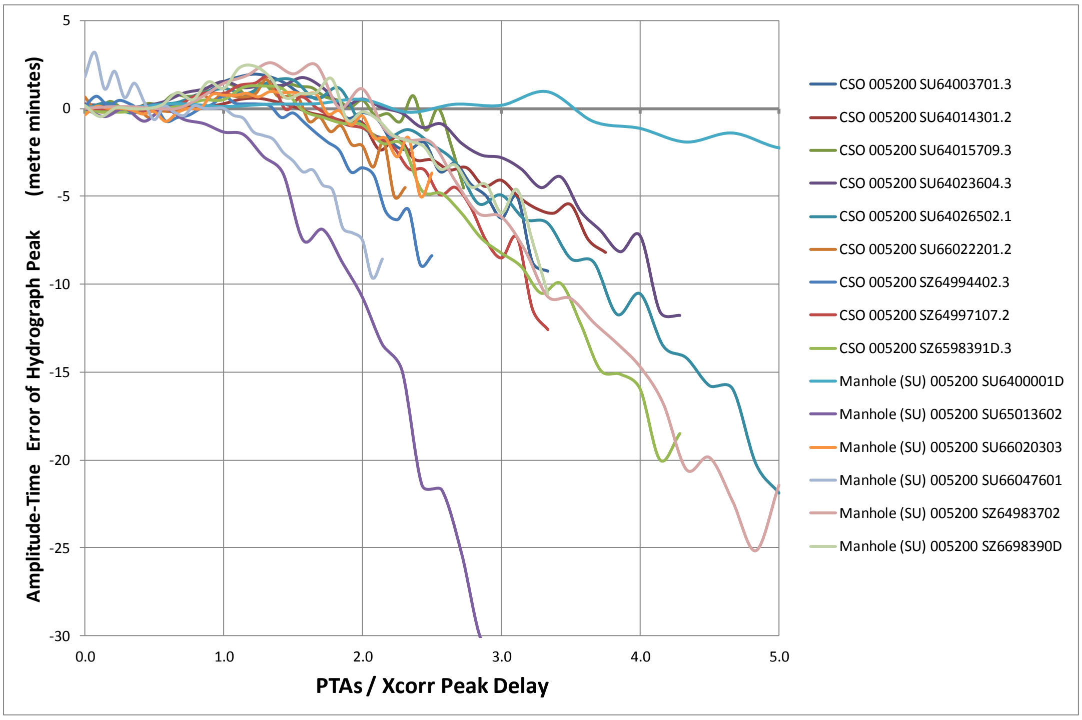

Figure 9. TA_{err} scores versus ratio of Prediction Timestep Advance to ToC for 5-yr, 2-hr event for 16-nodes from Portsmouth catchment

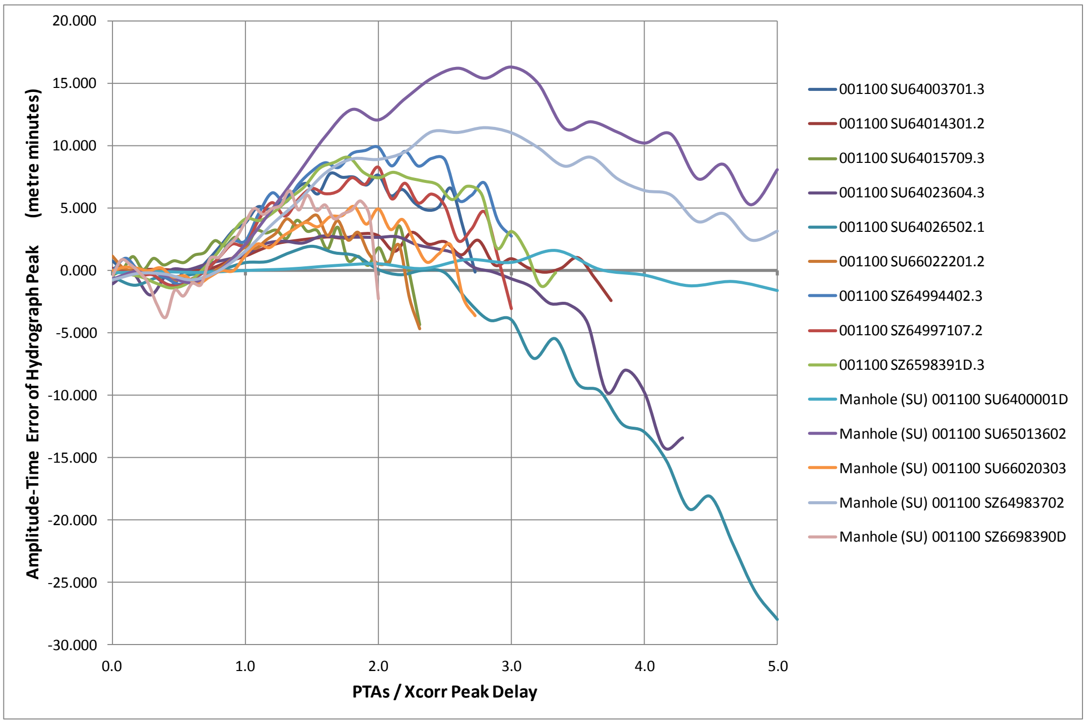

Figure 10. TA_{err} scores versus ratio of Prediction Timestep Advance to ToC for 1-yr, 1-hr event for 16-nodes from Portsmouth catchment

4. CONCLUSIONS

The results clearly demonstrate that acceptable performance for multi-node urban flood prediction can be achieved using single ANNs. They are able to exploit the similarities between the flood response hydrographs at the various nodes as illustrated by an ANN with 16 output nodes operating well with as few as 20 hidden units. At the same time, they are able to accommodate a range of times-of-concentration for the modelled nodes, which in this case spans a range of delays from 6 to 35 minutes, a ratio of 1:6. Corani & Guariso (2005) used pruning of hidden nodes to analyse the effect of each one effectively specialising in modelling different aspects of the overall ANN response. It is possible that these sorts of effect are present here. Further work is needed to analyse this.

The timing trial also clearly shows that use of lagged-input feedforward ANNs based on actual rainfall (instantaneous intensity and cumulative during event) as input signals is limited to prediction advances not greater than ToC for each node modelled. A physical explanation for this is that ToC is the length of time it takes for rainfall on the furthest (upstream) part of the catchment to arrive at the node. Effectively, trying to predict flooding beyond this advance means that there is no longer any relevant information in the actual rainfall input signals, since the relevant rainfall will not have started yet.

Because ToC's for urban drainage tend to be less than the required 2-hours for operationally useful forecasts (Einfalt et al., 2004), it will generally be necessary to use predictions of rainfall (nowcasting) in order to achieve these. However, such models have an opportunity to augment prediction capability by using the ToC times described in this paper.

ANNs produce deterministic rather than probabilistic predictions, but this can be an advantage as no assumptions about prior probability distributions of signals are necessary. In this case study, the MSE performance metric was used for training the ANNs. However, for urban flooding, perhaps the most important criterion is ability to predict the most extreme (high-impact) events most accurately. Perhaps it may be possible to aggregate the timing-amplitude error metric used here with the MSE or NSEC metric during training. This may improve prediction of the highest impact events and avoid the effects seen here of underprediction of the highest hydrograph peaks. Further work is needed.

5. ACKNOWLEDGEMENTS

The authors would like to thank Jemma Bennett and Martin Osborne of Mouchel for provision of the rainfall profiles and InfoWorks results used as target data. Richard Kellagher of HR Wallingford provided valuable project coordination and guidance. Thanks also to colleagues, Drs. Albert Chen and Michael Hammond for valuable advice.

6. REFERENCES

Amin, S.M., Wollenberg, B.F., (2005). Toward a smart grid: power delivery for the 21st century. *IEEE Power and Energy Magazine* 3, 34–41.

Anctil, F., Michel, C., Perrin, C., Andréassian, V., (2004). A soil moisture index as an auxiliary ANN input for stream flow forecasting. *Journal of Hydrology* 286, 155–167.

Battiti, R., (1992). First-and second-order methods for learning: between steepest descent and Newton’s method. *Neural Computation* 4, 141–166.

Bishop, C., (2008). *Neural Networks for Pattern Recognition*. OUP, Oxford, UK.

Bowden, G.J., Dandy, G.C., Maier, H.R., (2005). Input determination for neural network models in water resources applications. Part 1—background and methodology. *Journal of Hydrology* 301, 75–92.

Butler, D., Davies, J., (2004). Time of Concentration, in: *Urban Drainage*. Taylor & Francis, pp. 249–257.

Campolo, M., (2003). Artificial neural network approach to flood forecasting in the River Arno. *Hydrological Sciences*, 48(3) 381–398.

Corani, G., Guariso, G., (2005). An application of pruning in the design of neural networks for real time flood forecasting. *Neural Computing and Applications* 14, 66–77.

Duncan, A., Chen, A.S., Keedwell, E., Djordjevic, S., Savic, D.A., (2011). Urban flood prediction in real-time from weather radar and rainfall data using artificial neural networks, in: *IAHS Red Book* series no. 351, 58. Presented at the *Weather Radar and Hydrology International Symposium, International Association of Hydrological Sciences*, Exeter, UK.

Duncan, A.P., Chen, A.S., Keedwell, E.C., Djordjevic, S., Savic, D.A., (2013). RAPIDS: Early Warning System for Urban Flooding and Water Quality Hazards (Extended Abstract), in: *AISB 2013*. Presented at the *Artificial Intelligence and Simulation of Behaviour Conference; Machine Learning in Water Systems Symposium, AISB*, University of Exeter.

Einfalt, T., Arnbjerg-Nielsen, K., Golz, C., Jensen, N.-E., Quirmbach, M., Vaes, G., Vieux, B., (2004). Towards a roadmap for use of radar rainfall data in urban drainage. *Journal of Hydrology* 299 186–202.

European Commission, (2006). European SmartGrids technology platform: vision and strategy for europe's electricity networks of the future. *Directorate for Research* EUR 22040.

Fernando, T., Maier, H.R., Dandy, G.C., May, R., (2005). Efficient selection of inputs for artificial neural network models, in: Proc. of MODSIM 2005 *International Congress on Modelling and Simulation*: Modelling and Simulation Society of Australia and New Zealand.

FRMRC2, (2011). Flood Risk Management Research Consortium Website. http://www.floodrisk.org.uk/ (accessed 6 August 2013)

Hagan, M.T., Menhaj, M.-B., (1994). Training feedforward networks with the Marquardt algorithm. *IEEE Transactions on Neural Networks* 5, 989–993.

Han, D., Kwong, T., Li, S., (2007). Uncertainties in real-time flood forecasting with neural networks. *Hydrological Processes* 21, 223–228.

Heilig, G.K., (2012). World Urbanization Prospects The 2011 Revision. Presentation at the *Center for Strategic and International Studies (CSIS)* June, Washington, DC.

Innovyze, 2012. InfoWorks CS. Innovyze. http://www.innovyze.com/products/infoworks_cs/ (accessed 11 June 2012)

Ivakhnenko, A.G., (1971). Polynomial Theory of Complex Systems. *IEEE Transactions on Systems, Man and Cybernetics* SMC-1, 364–378.

Luk, K.C., Ball, J.E., Sharma, A., (2000). A study of optimal model lag and spatial inputs to artificial neural network for rainfall forecasting. *Journal of Hydrology* 227, 56–65.

Møller, M.F., (1993). A scaled conjugate gradient algorithm for fast supervised learning. *Neural Networks* 6, 525–533.

Moriasi, D.N., Arnold, J.G., Van Liew, M.W., Bingner, R.L., Harmel, R.D., Veith, T.L., (2007). Model evaluation guidelines for systematic quantification of accuracy in watershed simulations. *Transactions of the Asabe* 50, 885–900.

Nash, Je., Sutcliffe, J.V., (1970). River flow forecasting through conceptual models part I—A discussion of principles. *Journal of hydrology* 10, 282–290.

Rumelhart, D.E. and M.J.L., (1986). *Parallel Distributed Processing - Explorations in the Microstructure of Cognition*. MIT Press, Cambridge MA.

Savić, D.A., Bicik, J., Morley, M.S., Duncan, A., Kapelan, Z., Djordjevic, S., Keedwell, E.C., (2013). Intelligent Urban Water Infrastructure Management. *JIISc, Water Management in Changing Environment* 93, 319–335.

Schellart, A., Ochoa, S., Simões, N., Wang, L.P., Rico-Ramirez, M., Liguori, S., Duncan, A., Chen, A.S., Keedwell, E., Djordjević, S., others, (2011). Urban pluvial flood modelling with real time rainfall information–UK case studies, in: *ICUD 2011*. Presented at the *12th International Conference on Urban Drainage, IWA*, Porto Alegre/Brazil.

Schellart, A.N.A., Rico-Ramirez, M.A., Liguori, S., Saul, A.J., (2009). QUANTITATIVE PRECIPITATION FORECASTING FOR A SMALL URBAN AREA: USE OF RADAR NOWCASTING, in: *8th INTERNATIONAL WORKSHOP on PRECIPITATION IN URBAN AREAS*. -, St Moritz, CH, pp. 22–26.

UKWIR, (2012). The Use of Artificial Neural Networks (ANNs) in Modelling Sewerage Systems for Management in Real Time: Volume 1 - Main Report (12/SW/01/2) (Project Final Report No. 12/SW/01/2). *UKWIR (UK Water Industry Reseach)*, London, UK.

Wang, P., Smeaton, A., Lao, S., O'Connor, E., Ling, Y., O'Connor, N., (2009). Short-Term Rainfall Nowcasting: Using Rainfall Radar Imaging. *Eurographics Ireland* pp.

Zoppou, C., (2001). Review of urban storm water models. *Environmental Modelling & Software* 16, 195–231.